

Quantum Electrodynamics in Media with Negative Refraction *

Jürgen Kästel and Michael Fleischhauer

Fachbereich Physik, Technische Universität Kaiserslautern, D-67663 Kaiserslautern, Germany

(Dated: August 9, 2018)

We consider the interaction of atoms with the quantized electromagnetic field in the presence of materials with negative index of refraction. Spontaneous emission of an atom embedded in a negative index material is discussed. It is shown furthermore that the possibility of a vanishing optical path length between two spatially separated points provided by these materials can lead to complete suppression of spontaneous emission of an atom in front of a perfect mirror even if the distance between atom and mirror is large compared to the transition wavelength. Two atoms put in the focal points of a lens formed by a parallel slab of ideal negative index material are shown to exhibit perfect sub- and superradiance. The maximum length scale in both cases is limited only by the propagation distance within the free-space radiative decay time. Limitations of the predicted effects arising from absorption, finite transversal extension and dispersion of the material are analyzed.

PACS numbers:

I. INTRODUCTION

Since the early days of quantum electrodynamics it is well-known and appreciated that the radiative decay of an isolated atom as well as the radiative interaction between different atoms can be strongly affected by the environment. As first noted by E.M. Purcell [1, 2] the presence of conducting walls can strongly accelerate or suppress spontaneous emission. Inhibited emission [3], enhanced decay [4], and the suppression of blackbody absorption [5, 6] have been observed with Rydberg atoms in cavity systems. Alterations of the spontaneous emission rate have also been observed near dielectric interfaces [7] and in quantum-well structures [8]. Furthermore photonic band-gap materials with an engineered density of states of the radiation field can lead to suppression or acceleration of spontaneous decay [9, 10].

In this paper we discuss QED effects of single atoms and pairs of atoms in the presence of artificial materials showing negative refraction. Negative index materials were first predicted by V. Veselago [11], who showed that simultaneous negative values of the dielectric permittivity ϵ and the magnetic permeability μ imply a negative index of refraction. These so-called left-handed materials have attracted a lot of attention, when J. Pendry noticed that the possibility of a vanishing optical path length between two separated points using media with a negative index of refraction allows for a perfect lens with a resolution not limited by diffraction [12]. Such a lens formed by an infinite parallel slab of lossless left-handed material of thickness d collects all plane waves from a point source on one side of the slab in a focal point on the other side. If the refractive index of the material is $n = -1$,

the distance between the two focal points is $2d$, while the optical path between them vanishes. We will show here that the same effect can lead to a drastic modification of the radiative decay of a two-level atom placed in front of a conducting surface (Purcell effect) and the radiative interaction between two atoms even if the involved distances are large compared to the resonance wavelength. We show that spontaneous emission from an atom with distance $2d$ from the surface of a perfect mirror can be completely suppressed for dipole orientations in the plane of the mirror, if the space between atom and mirror contains a slab of $n = -1$ material with thickness d . With this an effect otherwise occurring only within a distance small compared to the transition wavelength would be observable for macroscopic distances. We will show furthermore that two atoms put into the focal points of an ideal Veselago-Pendry lens behave as if both would be in the same position i.e. they show perfect Dicke-sub and superradiance [13].

After summarizing the basic properties of left-handed materials and analyzing the conditions for their existence for the case of realistic i.e. causal, and in general lossy magneto-dielectrics in Sec.II, we will discuss the alteration of the spontaneous emission rate of an atom embedded in a left-handed material in Sec.III. It will be shown that the modification of the spontaneous emission rate due to the changed density of states is not anymore given by the index of refraction n as in dielectric materials [14], but by the product μn , which remains positive also for lossless negative-index materials [15]. We will then analyze the radiative decay of a single two-level atom in front of a perfect mirror with a layer of negative index material in Sec.IV and the radiative coupling of two atoms in the focal points of a Veselago-Pendry lens in Sec.V. Finally in Sec.VI we will discuss limitations due to finite absorption, a finite transversal extension of the lens as well as due to dispersion, which necessarily accompanies negative refraction.

*This paper is dedicated to the 70th birthday of Herbert Walther whose pioneering experimental work on cavity quantum electrodynamics with Rydberg atoms has sharpened our understanding of the fundamentals of light-matter interaction.

II. ELECTRODYNAMICS OF MEDIA WITH NEGATIVE REFRACTIVE INDEX

Macroscopic electrodynamics in linear, isotropic media is completely characterized by the two material functions dielectric permittivity ε and magnetic permeability μ . ε and μ relate the vector of the polarization \mathbf{P} to that of the electric field \mathbf{E} and, correspondingly, the vector of magnetization \mathbf{M} to that of the magnetic field \mathbf{B} . The most general expressions for \mathbf{P} and \mathbf{M} in linear isotropic magneto-dielectrics read:

$$\mathbf{P}(\mathbf{r}, t) = \varepsilon_0 \int_{-\infty}^{\infty} d\tau \chi_D(\mathbf{r}, \tau) \mathbf{E}(\mathbf{r}, t - \tau) \quad (1)$$

and

$$\mathbf{M}(\mathbf{r}, t) = \kappa_0 \int_{-\infty}^{\infty} d\tau \chi_M(\mathbf{r}, \tau) \mathbf{B}(\mathbf{r}, t - \tau) \quad (2)$$

where $\kappa_0 = 1/\mu_0$. χ_D and χ_M are the electric and magnetic susceptibilities respectively. For causality the susceptibilities have to be zero for $\tau < 0$. The dielectric permittivity $\varepsilon(\omega)$ then reads

$$\varepsilon(\mathbf{r}, \omega) = 1 + \int_0^{\infty} d\tau \chi_D(\mathbf{r}, \tau) e^{i\omega\tau}. \quad (3)$$

Correspondingly the magnetic permeability $\mu = 1/\kappa$ is given by

$$\kappa(\mathbf{r}, \omega) = 1 - \int_0^{\infty} d\tau \chi_M(\mathbf{r}, \tau) e^{i\omega\tau}. \quad (4)$$

Causality requires that the poles of $\varepsilon(\omega)$ and $\mu(\omega)$ are in the lower half of the complex plane. $\varepsilon(\omega)$ and $\mu(\omega)$ usually have a resonance structure in ω -space, e.g.

$$\varepsilon(\omega) = 1 + \frac{\omega_{Pe}^2}{\omega_{Te}^2 - \omega^2 - i\omega\gamma_e} \quad (5)$$

and

$$\mu(\omega) = 1 + \frac{\omega_{Pm}^2}{\omega_{Tm}^2 - \omega^2 - i\omega\gamma_m}. \quad (6)$$

For sufficient strength of the resonance, i.e. for ω_{Pe}, ω_{Pm} large, both $\text{Re}[\varepsilon]$ and $\text{Re}[\mu]$ may become negative for certain frequencies.

Suppose that at a particular frequency $\varepsilon = \mu = -1$ holds. Then the question arises what are the implications on the refractive index $n(\mathbf{r}, \omega)$? From the definition of $n(\mathbf{r}, \omega)$

$$n(\mathbf{r}, \omega)^2 = \varepsilon(\mathbf{r}, \omega) \cdot \mu(\mathbf{r}, \omega) \quad (7)$$

one might conclude

$$n = \sqrt{\varepsilon \cdot \mu} = \sqrt{(-1) \cdot (-1)} = \sqrt{1} = 1. \quad (8)$$

However, as pointed out by Veselago [11], since ε and μ are complex functions, one has to decide which complex

root to take. Noting, that the imaginary part of $n(\mathbf{r}, \omega)$ characterizes the absorption of the medium, for a passive medium $\text{Im}[n(\mathbf{r}, \omega)] \geq 0$ should hold, which fixes the root. As can be seen from figure 1 the correct choice is

$$n(\mathbf{r}, \omega) = \sqrt{|\varepsilon(\mathbf{r}, \omega)| \cdot |\mu(\mathbf{r}, \omega)|} \cdot \exp \left[+\frac{i}{2} \left(\text{arccot} \frac{\varepsilon_R(\mathbf{r}, \omega)}{\varepsilon_I(\mathbf{r}, \omega)} + \text{arccot} \frac{\mu_R(\mathbf{r}, \omega)}{\mu_I(\mathbf{r}, \omega)} \right) \right]. \quad (9)$$

Here ε_R, μ_R and ε_I, μ_I denote real and imaginary parts of ε and μ respectively. With this one finds for the case

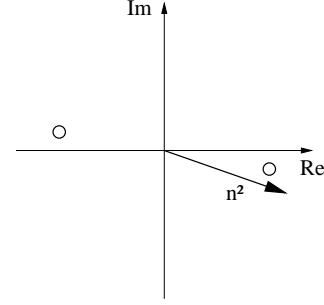


FIG. 1: n^2 for $\text{Re}[\varepsilon], \text{Re}[\mu]$ both being negative. The two possible complex square roots are indicated by circles

of $\varepsilon = \mu = -1$:

$$n = \lim_{\varepsilon_I, \mu_I \searrow 0} \exp \left[\frac{i}{2} \left(\text{arccot} \frac{-1}{\varepsilon_I} + \text{arccot} \frac{-1}{\mu_I} \right) \right] = -1. \quad (10)$$

It is easy to see from eq.(9) that a negative real part of the refractive index occurs if and only if [16]

$$\pi \geq \text{arccot} \left(\frac{\varepsilon_R}{\varepsilon_I} \right) + \text{arccot} \left(\frac{\mu_R}{\mu_I} \right) > \pi/2. \quad (11)$$

In fig.2 we have illustrated the frequency dependence of the index of refraction for the single-resonance model given in (5,6). For frequencies around $\omega = 1.05\omega_{Te}$ the negativity of $\text{Re}[n]$ is clearly recognizable.

The example of figure 2 shows a strong dispersion of the material functions $\varepsilon(\omega)$ and $\mu(\omega)$. In fact, as pointed out already by Veselago, this is a general property of negative-index materials. Considering the energy of the electromagnetic field in a non-dispersive medium

$$w = \varepsilon \mathbf{E}^2 + \mu \mathbf{H}^2 \quad (12)$$

one recognizes that negative values of ε and μ would lead to a negative energy. Therefore a negative index of refraction is necessarily associated with dispersion, in which case the energy of the electromagnetic field reads

$$w = \text{Re} \left[\frac{d(\omega\varepsilon)}{d\omega} \right] \mathbf{E}^2 + \text{Re} \left[\frac{d(\omega\mu)}{d\omega} \right] \mathbf{H}^2 \quad (13)$$

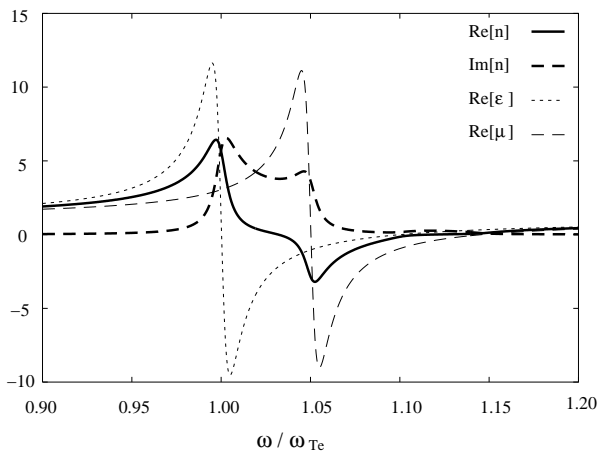


FIG. 2: $\text{Re}[n(\omega)], \text{Im}[n(\omega)], \text{Re}[\varepsilon(\omega)]$ and $\text{Re}[\mu(\omega)]$ using eqs.(5) and (6). Parameters: $\omega_{Pe} = \omega_{Pm} = 0,46\omega_{Te}$; $\omega_{Tm} = 1,05\omega_{Te}$; $\gamma_e = \gamma_m = 0,01\omega_{Te}$.

which is positive even for negative ε and μ if the dispersion is normal and sufficiently large, such that

$$\text{Re} \left[\frac{d(\omega\varepsilon)}{d\omega} \right] \geq 0, \quad \text{and} \quad \text{Re} \left[\frac{d(\omega\mu)}{d\omega} \right] \geq 0. \quad (14)$$

In the following we want to discuss some of the peculiar aspects of light propagation in negative-index materials. Making use of the boundary conditions between media with positive and negative refractive indexes, namely $\mathbf{E}^\perp, \mathbf{H}^\perp$ being continuous as well as $\mathbf{D}^\parallel, \mathbf{B}^\parallel$, one finds that an incident plane wave is refracted to the same side of the normal as shown in figure 3. This behavior is fully consistent with Snells law

$$\frac{n_2}{n_1} = \frac{\sin(\alpha)}{\sin(\beta)}. \quad (15)$$

One striking feature of negative refraction is, that the wave vector of the refracted wave \mathbf{k}^r points backward which is due to conservation of momentum parallel to the surface. As a result the vectors $\mathbf{k}, \mathbf{E}, \mathbf{H}$ form a left-handed tripod instead of the usual right-handed one. Materials with a negative index of refraction are therefore also called left-handed media (LHM).

On the other hand the Poynting vector $\mathbf{S} = \mathbf{E} \times \mathbf{H}$ clearly forms a right-handed tripod with \mathbf{E} and \mathbf{H} and therefore points in the correct direction, namely away from the surface, as it should be due to conservation of energy (dashed arrows in fig. 3).

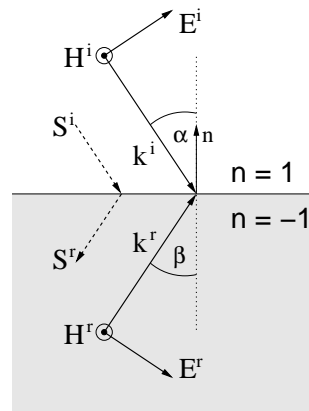


FIG. 3: Boundary between positive and negative refraction. In a material with a negative refractive index, the refracted wave goes to negative angles.

Besides strong influences on Doppler and Cherenkov effects [11], the most prominent effect of the negative refraction is probably the so-called perfect lens formed by a slab of a LHM. It was Veselago [11] who, when first studying the properties of lenses formed by a left-handed material, found that an infinitely extended slab of a LHM collects all plane waves coming from a point source not too far away from the surface in a focal point on the other side of the slab (fig. 4). For a slab of thickness

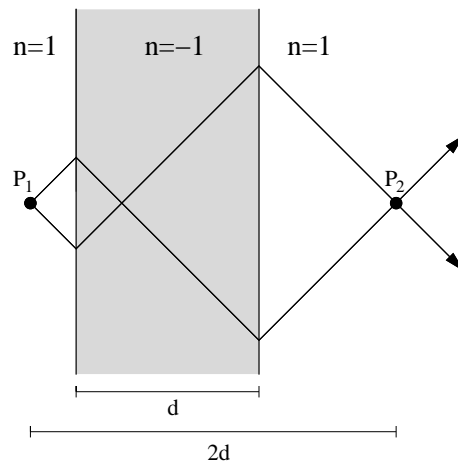


FIG. 4: Perfect lens formed by a infinitely extended slab of a LHM. The optical length between the foci P_1 and P_2 is zero.

d the distance between the two focal points is $d(1 - n)$, where n is the refractive index of the LHM. Noting that the optical path-length between points P_1 and P_2

$$l^{\text{opt.}} = (d(1 - n) - d) + nd = 0, \quad (16)$$

the perfection of the lens becomes clear. The lens simulates point P_2 to be at the same spatial position as point P_1 . Traveling a zero path no information about the source can get lost, including that contained in the

evanescent waves. Therefore the perfect lens allows an unlimited resolution of the source [12].

III. SPONTANEOUS EMISSION OF AN ATOM EMBEDDED IN A MEDIUM WITH NEGATIVE REFRACTION

It is a well known fact, that the natural linewidth Γ of a dipole allowed transition is not an intrinsic feature of an atom, but depends on the local environment. Based on an analysis of the density of states of the radiation field Nienhuis and Alkemade predicted for an atom embedded in a homogeneous transparent dielectric with refractive index n [14]

$$\Gamma = \Gamma_0 n, \quad (17)$$

where Γ_0 is the free-space decay rate:

$$\Gamma_0 = \frac{d^2 \omega_A^3}{3\pi \hbar \epsilon_0 c^3} \quad (18)$$

with d being the dipole moment and ω_A the atomic transition frequency. It was seen later on that eq.(17) does not give the correct behavior of Γ since the macroscopic description of the surrounding medium fails in the immediate environment of the probe atom. To correct this in leading order of the medium density, local-field corrections need to be included. Several models have been established for this. The one that best describes a substitutive probe atom in a cubic-lattice host is the so-called real-cavity-model [17] in which

$$\Gamma = n\Gamma_0 \mathcal{L}_{\text{real}}^2. \quad (19)$$

Here $\mathcal{L}_{\text{real}} = 3\epsilon/(2\epsilon + 1)$ is the Glauber-Lewenstein factor which accounts for near field effects. This model assumes the atom to be located at the center of a small empty cavity surrounded by the dielectric body which is treated macroscopically (see fig. 5).

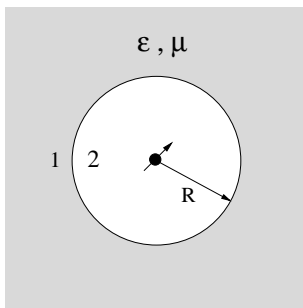


FIG. 5: Real-cavity model: the atom is located at the center of an empty cavity surrounded by the dielectric body.

When considering atoms embedded in negative index materials eqs.(17) and (19) are obviously not correct,

since Γ would become negative in this case. This is because these expressions are derived only for dielectric surroundings [17, 18], where the contribution of the magnetic dipoles of the material was neglected.

Following Fermis golden rule the rate of spontaneous emission of an electric dipole transition is given by the imaginary part of the retarded Greensfunction \mathbf{G} of the electric field at the position \mathbf{r}_A of the atom and at the transition frequency ω_A [15]

$$\Gamma = \frac{2\omega_A^2 d_i d_j}{\hbar \epsilon_0 c^2} \text{Im} [G_{ij}(\mathbf{r}_A, \mathbf{r}_A, \omega_A)]. \quad (20)$$

Here d_i is the Cartesian i th-component of the dipole moment. The influence of the surrounding on the mode structure is contained in the Greenstensor \mathbf{G} . Thus in order to include the effect of the magnetic dipoles of the left-handed medium, the Greenstensor needs to be calculated for the case of a magneto-dielectrics. Thus the solution of the equation

$$\left(\nabla_{\mathbf{r}} \times [\kappa(\mathbf{r}, \omega) \nabla_{\mathbf{r}} \times] - \frac{\omega^2}{c^2} \epsilon(\mathbf{r}, \omega) \right) \mathbf{G}(\mathbf{r}, \mathbf{r}', \omega) = \delta(\mathbf{r} - \mathbf{r}') \mathbf{1} \quad (21)$$

needs to be determined for given boundary conditions. Note the term $\kappa(\mathbf{r}, \omega) = 1/\mu(\mathbf{r}, \omega)$ which is absent in the pure dielectric case [18].

Since within the Glauber-Lewenstein model the atom is located in free space, the solution of (21) for the real-cavity (fig. 5) can be expressed as a sum of the free space Greensfunction and a scattering term accounting for the boundary to the magneto-dielectric:

$$\mathbf{G}(\mathbf{r}, \mathbf{r}') = \mathbf{G}^{\text{vac}}(\mathbf{r}, \mathbf{r}') + \mathbf{G}^s(\mathbf{r}, \mathbf{r}') \quad |\mathbf{r}|, |\mathbf{r}'| < R \quad (22)$$

with

$$\text{Im} [\mathbf{G}_{ij}^{\text{vac}}(\mathbf{r}, \mathbf{r}, \omega)] = \frac{k}{6\pi} \delta_{ij}, \quad k = \omega/c \quad (23)$$

and

$$\begin{aligned} \mathbf{G}^s(\mathbf{r}, \mathbf{r}') &= \frac{ik}{4\pi} \sum_{n=1}^{\infty} \sum_{m=0}^n \sum_{l=e,o}^n (2 - \delta_{0m}) \frac{2n+1}{n(n+1)} \frac{(n-m)!}{(n+m)!} \\ &\cdot \left[C_M^n(k) \mathbf{M}_{lmn}(\mathbf{r}, k) \mathbf{M}_{lmn}(\mathbf{r}', k) \right. \\ &\left. + C_N^n(k) \mathbf{N}_{lmn}(\mathbf{r}, k) \mathbf{N}_{lmn}(\mathbf{r}', k) \right]. \end{aligned} \quad (24)$$

Due to the symmetry of the geometry the scattering term can be expanded in a series of vector Bessel functions:

$$\mathbf{M}_{lmn}(\mathbf{r}, k) = \nabla \times [\psi_{lmn}(\mathbf{r}, k) \mathbf{r}], \quad (25)$$

$$\mathbf{N}_{lmn}(\mathbf{r}, k) = \frac{1}{k} \nabla \times \nabla \times [\psi_{lmn}(\mathbf{r}, k) \mathbf{r}], \quad (26)$$

$$\psi_{lmn}(\mathbf{r}, k) = j_n(kr) P_n^m(\cos \theta) f_l(m\phi), \quad (27)$$

f_l has the meaning of a cosine function for even l and of a sine function for l being odd. The j_n are spherical Bessel

functions of the first kind and the P_n^m associated Legendre polynomials. The rather lengthy expansion factors $\mathcal{C}_N^n(k)$ and $\mathcal{C}_M^n(k)$ are given in [19].

In the limit $\mathbf{r}, \mathbf{r}' \rightarrow 0$ all terms but that with \mathcal{C}_N^1 become zero. The rate of spontaneous emission of a 2-level atom embedded in a medium of arbitrary ε and μ then reads

$$\Gamma = \Gamma_0 \left(1 + \text{Re} [\mathcal{C}_N^1(\omega_A)] \right) \quad (28)$$

with

$$\begin{aligned} \mathcal{C}_N^1(\omega_A) = & e^{i\varrho} \left[i + \varrho(n+1) - i\varrho^2 n(n+1) \frac{\mu-n}{\mu-n^2} - \varrho^3 n^2 \frac{\mu-n}{\mu-n^2} \right] \\ & \cdot \left[i\varrho^2 n \left(\cos \varrho + in \frac{\mu-1}{\mu-n^2} \sin \varrho \right) - \varrho (\cos \varrho + in \sin \varrho) \right. \\ & \left. \sin \varrho + \varrho^3 (\mu \cos \varrho - in \sin \varrho) \frac{n^2}{\mu-n^2} \right]^{-1}. \end{aligned} \quad (29)$$

Here $\varrho = \frac{R\omega_A}{c}$ is the normalized radius of the cavity. This function can be shown to be strictly positive, as it should be for the rate of spontaneous emission. In the limit of vanishing imaginary parts of μ , ε , and n , eq.(28) reduces to

$$\Gamma = n\mu \Gamma_0 \left(\frac{3\varepsilon}{2\varepsilon+1} \right)^2 \quad (30)$$

which is the sought generalization of the formula of Glauber and Lewenstein (19) for pure dielectrics to the case of lossless but otherwise arbitrary magneto-dielectric media. For $\mu = 1$ equation (30) reduces to the dielectric case.

The influence of the LHM on the rate of spontaneous emission for a resonance model using the example of eqs.(5) and (6) is shown in figure 6. Because of the surrounding medium the natural linewidth in the vicinity of the resonance can be either strongly enhanced or suppressed.

IV. SUPPRESSION OF SPONTANEOUS EMISSION OF AN ATOM IN FRONT OF A MIRROR: MODIFIED PURCELL EFFECT

In this section the modification of the Purcell effect, i.e. the suppression of the spontaneous emission of an atom in front of a mirror by a medium with negative refraction will be discussed. For this we consider the setup shown in fig. 7. The atom is placed at a distance $2d$ from the surface of the perfect mirror and the space between atom and mirror is filled half by vacuum and half by a medium with $n = -1$.

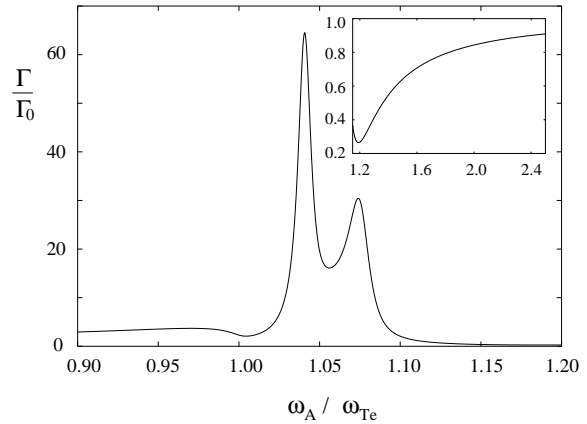


FIG. 6: Rate of spontaneous emission for the real-cavity model for the resonant functions (5) and (6). $\omega_{Pe} = \omega_{Pm} = 0,46\omega_{Te}$, $\omega_{Tm} = 1,05\omega_{Te}$ and $\gamma_e = \gamma_m = 0,01\omega_{Te}$

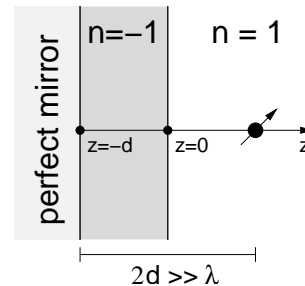


FIG. 7: Atom in front of a LHM attached to a mirror. The optical length between atom and mirror is zero. The spatial regions $z > 0$, $-d \leq z \leq 0$, and $z < -d$ are denoted by the numbers 0, 1, 2 respectively.

In the absence of the medium, the emission rate of the atom is significantly affected only if the distance between atom and mirror is small compared to the transition wavelength [20]. In this case the radiative decay for a transition with dipole moment parallel to the plane of the mirror vanishes, while that for an orthogonal dipole moment is enhanced by a factor 2. Since in the presence of the negative index material as in fig.7, the optical length of the path from the atom to the mirror equals zero, the question arises whether the LHM leads to properties comparable to the case of the atom sitting on the mirror surface. To obtain an answer to this we note, that the rate of spontaneous emission of an atom in a linear, isotropic but otherwise arbitrary environment is given by (20). Thus we only need to calculate the Greensfunction corresponding to the specific set-up.

The retarded Greensfunction corresponding to a slab with a homogeneous and linear magneto-dielectric medium can be calculated by a plane wave decomposition. Following [21] one finds for the two positions \mathbf{r} and

\mathbf{r}' in vacuum on the same side of the slab

$$\mathbf{G}^{00}(\mathbf{r}, \mathbf{r}', \omega) = \frac{i}{8\pi^2} \int d^2 k_{\perp} \frac{1}{k_z} \left[\begin{aligned} &(R^{\text{TE}} \hat{\mathbf{e}}(k_z) e^{i\mathbf{k}\cdot\mathbf{r}} + \hat{\mathbf{e}}(-k_z) e^{i\mathbf{K}\cdot\mathbf{r}}) \circ \hat{\mathbf{e}}(-k_z) e^{-i\mathbf{K}\cdot\mathbf{r}'} \\ &+ (R^{\text{TM}} \hat{\mathbf{h}}(k_z) e^{i\mathbf{k}\cdot\mathbf{r}} + \hat{\mathbf{h}}(-k_z) e^{i\mathbf{K}\cdot\mathbf{r}}) \circ \hat{\mathbf{h}}(-k_z) e^{-i\mathbf{K}\cdot\mathbf{r}'} \end{aligned} \right], \quad (31)$$

where $z \leq z'$ has been assumed. Since it is needed later, we also give the Greensfunction for \mathbf{r} and \mathbf{r}' being in vacuum on different sides of the slab

$$\mathbf{G}^{20}(\mathbf{r}, \mathbf{r}', \omega) = \frac{i}{8\pi^2} \int d^2 k_{\perp} \frac{1}{k_z} \left[\begin{aligned} &T^{\text{TE}} \hat{\mathbf{e}}(-k_z) e^{i\mathbf{K}\cdot\mathbf{r}} \circ \hat{\mathbf{e}}(-k_z) e^{-i\mathbf{K}\cdot\mathbf{r}'} \\ &+ T^{\text{TM}} \hat{\mathbf{h}}(-k_z) e^{i\mathbf{K}\cdot\mathbf{r}} \circ \hat{\mathbf{h}}(-k_z) e^{-i\mathbf{K}\cdot\mathbf{r}'} \end{aligned} \right]. \quad (32)$$

The superscripts 0, 1, 2 at the Greensfunctions denote the zones of positions \mathbf{r} and \mathbf{r}' : $z > 0$, $-d \leq z \leq 0$, and $z < -d$ respectively. For later convenience \mathbf{G}^{20} is given under the assumption of medium 2 being vacuum. We here have used the definitions $k^2 = \omega^2/c^2$, $k_z = \sqrt{k^2 - k_{\perp}^2}$ and $d^2 k_{\perp} = dk_x dk_y$. Furthermore $\mathbf{K} \equiv k_x \hat{\mathbf{x}} + k_y \hat{\mathbf{y}} - k_z \hat{\mathbf{z}}$ and we have introduced the orthogonal unit vectors $\hat{\mathbf{e}} = \mathbf{k} \times \hat{\mathbf{z}} / |\mathbf{k} \times \hat{\mathbf{z}}|$ and $\hat{\mathbf{h}} = p \hat{\mathbf{e}} \times \mathbf{k} / |k|$, where $p = 1$ for a normal medium and $p = -1$ for a LHM. $R^{\text{TE}}, R^{\text{TM}}$ and $T^{\text{TE}}, T^{\text{TM}}$ are the reflection and transmission functions of the 3-layer medium for transverse electric and transverse magnetic modes. They read

$$R^{\text{TE}} = \frac{R_{01} + R_{12} e^{i2k_{1z}d}}{1 + R_{01}R_{12} e^{i2k_{1z}d}}, \quad (33)$$

$$R^{\text{TM}} = \frac{S_{01} + S_{12} e^{i2k_{1z}d}}{1 + S_{01}S_{12} e^{i2k_{1z}d}}, \quad (34)$$

and correspondingly

$$T^{\text{TE}} = \frac{2\mu k_z}{\mu k_z + k_{1z}} \frac{1 + R_{12}}{1 + R_{01}R_{12} e^{i2k_{1z}d}} e^{i(k_{1z} - k_z)d}, \quad (35)$$

$$T^{\text{TM}} = \frac{2\varepsilon k_z}{\varepsilon k_z + k_{1z}} \frac{1 + S_{12}}{1 + S_{01}S_{12} e^{i2k_{1z}d}} e^{i(k_{1z} - k_z)d}. \quad (36)$$

Here $k_{1z} = \sqrt{k_1^2 - k_{\perp}^2}$ and $k_1^2 = \varepsilon(\omega)\mu(\omega)\omega^2/c^2$. R_{ij} and S_{ij} are the reflection coefficients at the boundaries between media i and j for TE and TM modes respectively.

$$R_{ij} = \frac{\mu_j k_{iz} - \mu_i k_{jz}}{\mu_j k_{iz} + \mu_i k_{jz}}, \quad S_{ij} = \frac{\varepsilon_j k_{iz} - \varepsilon_i k_{jz}}{\varepsilon_j k_{iz} + \varepsilon_i k_{jz}}. \quad (37)$$

Setting $R_{12} = -1$ and $S_{12} = 1$ to account for the perfect mirror, we get the natural linewidth by substituting the corresponding result for \mathbf{G}^{00} into

$$\Gamma = \frac{2\omega_A^2 d_i d_j}{\hbar \varepsilon_0 c^2} \text{Im} [\mathbf{G}_{ij}^{00}(\mathbf{r}_A, \mathbf{r}_A, \omega_A)]. \quad (38)$$

The result is shown in figure 8 for the case of the atomic dipole moment being parallel to the surface of the mirror. The thickness of the LHM is set to $d = 100 \frac{\lambda}{2\pi}$. When the atom is put at a distance d before the LHM, which we want to denote as focal point, the rate of spontaneous emission is completely suppressed:

$$\Gamma_{\text{focus}}^{\parallel} = 0. \quad (39)$$

The spatial dependence of the linewidth shown in figure 8 is the same as for an atom in front of a mirror located at $z = 0$ without LHM [20]. For atomic dipoles with

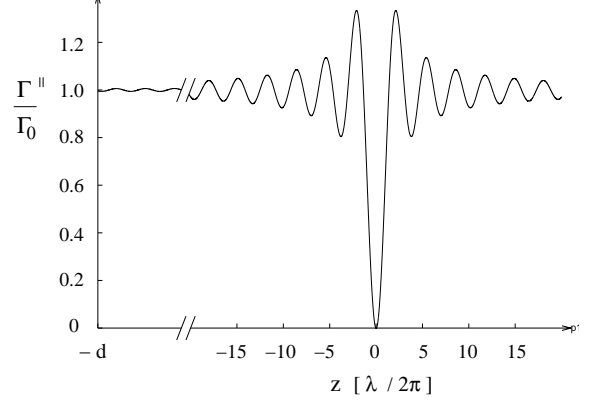


FIG. 8: Spatial dependence of the normalized rate of spontaneous emission $\Gamma^{\parallel}(z)/\Gamma_0$ for dipole parallel to mirror surface. z is the spatial shift in z -direction of the atom out of its focus; d is the distance from the focus to the surface of the LHM.

orthogonal orientation to the mirror, the spatial dependence is also the same as in the case of no LHM but the mirror being at $z = 0$ position (see [20]). In the focus this leads to an enhancement of the decay rate by a factor of 2:

$$\Gamma_{\text{focus}}^{\perp} = 2\Gamma_0 \quad (40)$$

The behavior shown in fig.8 can be understood in the following way: The combination of layers of vacuum ($n = +1$) and of negative index material ($n = -1$) with equal thickness d makes the space between atom and mirror to appear of zero (optical) length. Thus the atom in the focal point is equivalent to the atom being on the mirror surface. This result suggests the possibility to experimentally study spontaneous emission suppression of atoms near a mirror without the necessity of actually putting the atoms on the surface.

V. SUB- AND SUPERRADIANCE OVER MACROSCOPIC DISTANCES

The observation of the last section, that a combination of a layer of positive and negative refraction can make a

spatial volume to appear to have vanishing optical thickness, suggests a different interesting application. If two atoms are put in the focal points of a Veselago-Pendry lens, as indicated in fig.9, they should show a radiative coupling with a strength as if they would be at the same position in space.

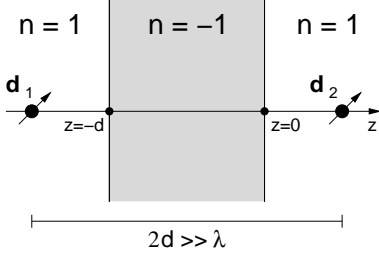


FIG. 9: two atoms put into the focal points of a Veselago-Pendry lens with $n = -1$. Focal points are all pairs of positions at the two sides of the slab with distance $2d$. The spatial regions $z > 0$ (vacuum), $-d \leq z \leq 0$ (LHM), and $z < -d$ (vacuum) are denoted by the numbers 0, 1, 2 respectively.

We now want to analyze this situation in detail. For this we start with the interaction Hamiltonian of two atoms at positions \mathbf{r}_1 and \mathbf{r}_2 with the quantized electric field $\hat{\mathbf{E}}$ in dipole and rotating-wave approximation:

$$H_{\text{WW}} = -\hat{\mathbf{E}}(\mathbf{r}_1)\hat{\mathbf{d}}_1 - \hat{\mathbf{E}}(\mathbf{r}_2)\hat{\mathbf{d}}_2. \quad (41)$$

Eliminating the electromagnetic field using the usual Born-Markov approximations leads to a two-atom Liouville equation of the form

$$\begin{aligned} \dot{\rho} = & -\frac{i}{\hbar} [\hat{H}_0, \rho] \\ & - \sum_{k,l=1}^2 \frac{\Gamma(\mathbf{r}_k, \mathbf{r}_l)}{2} (\hat{\sigma}_l^\dagger \hat{\sigma}_k \rho + \rho \hat{\sigma}_l^\dagger \hat{\sigma}_k - 2\hat{\sigma}_k \rho \hat{\sigma}_l^\dagger) \\ & + \frac{i}{\hbar} \sum_{k,l=1}^2 \delta\omega(\mathbf{r}_k, \mathbf{r}_l) [\hat{\sigma}_l^\dagger \hat{\sigma}_k, \rho], \end{aligned} \quad (42)$$

where $\hat{\sigma}_l = |1\rangle_l \langle 2|$ is the atomic flip operator of the l th atom from the lower state $|1\rangle$ to the upper state $|2\rangle$. The second and third term in (42) describe the spontaneous emission and Lamb-shift of the two individual atoms with decay rates $\Gamma(\mathbf{r}_i, \mathbf{r}_i)$ and respective level shifts $\delta\omega(\mathbf{r}_i, \mathbf{r}_i)$, ($i = 1, 2$). However they also contain terms describing the radiative interaction between the atoms containing a dissipative cross coupling proportional to $\Gamma(\mathbf{r}_1, \mathbf{r}_2)$ and a conditional level shift proportional to $\delta\omega(\mathbf{r}_1, \mathbf{r}_2)$. The single-atom and cross-coupling rates are given by an expression similar to (20):

$$\Gamma(\mathbf{r}_k, \mathbf{r}_l) = \frac{2\omega_A^2 d_i d_j}{\hbar \epsilon_0 c^2} \text{Im} [G_{ij}(\mathbf{r}_k, \mathbf{r}_l, \omega_A)]. \quad (43)$$

The level shifts read

$$\delta\omega(\mathbf{r}_k, \mathbf{r}_l) = \frac{d_i d_j}{\hbar \pi \epsilon_0} \mathcal{P} \int_0^\infty d\omega \frac{\omega^2}{c^2} \frac{\text{Im} [G_{ij}(\mathbf{r}_k, \mathbf{r}_l, \omega)]}{\omega - \omega_A}. \quad (44)$$

The single-atom Lamb shift $\delta\omega(\mathbf{r}_i, \mathbf{r}_i)$ is not accurately described within the present theory and will be ignored in the following. One recognizes from (43) and (44) that the radiative interaction between the two atoms is determined by the imaginary part of the retarded Greensfunction between the positions \mathbf{r}_1 and \mathbf{r}_2 of the two atoms. In free space the value of \mathbf{G} rapidly decreases if the relative distance $|\mathbf{r}_1 - \mathbf{r}_2|$ becomes larger than the transition wavelength λ . Consequently the radiative interaction is negligible except for very small distances. As will be shown now this situation changes if the atoms are put into the focal points of a Veselago-Pendry lens.

In order to see the effect of the radiative coupling it is convenient to use as a basis for the two-atom system besides the total ground state $|11\rangle$ and the doubly-excited state $|22\rangle$ the symmetric and antisymmetric combinations of one atom being excited ($|2\rangle$) and one atom being in its ground state ($|1\rangle$):

$$|s\rangle \equiv \frac{1}{\sqrt{2}} (|12\rangle + |21\rangle), \quad (45)$$

$$|a\rangle \equiv \frac{1}{\sqrt{2}} (|12\rangle - |21\rangle). \quad (46)$$

In terms of these basis states we arrive at the following density-matrix equation

$$\dot{\rho}_{22} = -2\Gamma_{11}\rho_{22}, \quad (47)$$

$$\dot{\rho}_{ss} = -(\Gamma_{11} + \Gamma_{12})\rho_{ss} + (\Gamma_{11} + \Gamma_{12})\rho_{22}, \quad (48)$$

$$\dot{\rho}_{aa} = -(\Gamma_{11} - \Gamma_{12})\rho_{aa} + (\Gamma_{11} - \Gamma_{12})\rho_{22}, \quad (49)$$

$$\dot{\rho}_{11} = +(\Gamma_{11} + \Gamma_{12})\rho_{ss} + (\Gamma_{11} - \Gamma_{12})\rho_{aa}, \quad (50)$$

where we have disregarded the level shifts and Γ_{ij} is a short notation for $\Gamma(\mathbf{r}_i, \mathbf{r}_j)$. One recognizes from the above equations that the decay channels through the symmetric and antisymmetric superpositions differ by the cross-coupling contribution $\pm\Gamma_{12}$. If the two atoms are in free space at the same point $\Gamma_{12} = \Gamma_{11} = \Gamma_{22}$. In this case the antisymmetric state does not decay at all, while the symmetric one decays with twice the single-atom decay rate. This is the situation of Dicke sub- and superradiance [13].

Let us now calculate the rates Γ_{11} , Γ_{22} and Γ_{12} i.e. the imaginary part of the Greensfunction for the situation of fig.9. Since at the boundary between vacuum ($n = +1$) and LHM ($n = -1$) there is no reflection, i.e. $R^{TE} = R^{TM} = 0$ one finds for the case of both positions being on the left side of the lens (region "0")

$$\begin{aligned} \text{Im} [G_{\mu\mu}^{00}(\mathbf{r}, \mathbf{r})] = & \text{Im} \frac{i}{8\pi^2} \int_0^\infty dk_\perp \frac{k_\perp}{\sqrt{k^2 - k_\perp^2}} \\ & \left((1 + R^{TE} e^{i\sqrt{k^2 - k_\perp^2} d}) \pi \right. \\ & \left. + R^{TM} e^{i\sqrt{k^2 - k_\perp^2} d} \pi \left(\frac{k_\perp^2}{k^2} - 1 \right) + \pi \left(1 - \frac{k_\perp^2}{k^2} \right) \right) \\ = & \frac{k}{6\pi}. \end{aligned} \quad (51)$$

The same result holds of course for both positions being on the right side of the lens (region “2”). A corresponding calculation for \mathbf{r} being on the left side (region “0”) and \mathbf{r}' being the other focal point of the lens $\mathbf{r} + 2d\mathbf{e}_z$ yields

$$\begin{aligned} \text{Im} [\mathbf{G}_{11}^{20}(\mathbf{r}, \mathbf{r} + 2d\mathbf{e}_z)] &= \text{Im} \frac{i}{8\pi^2} \int_0^\infty dk_\perp \frac{k_\perp}{\sqrt{k^2 - k_\perp^2}} \\ &\cdot e^{i2\sqrt{k^2 - k_\perp^2}d} \cdot \left(T^{TE} \pi + T^{TM} \pi \left(1 - \frac{k_\perp^2}{k^2} \right) \right) \\ &= \frac{k}{6\pi}, \end{aligned} \quad (52)$$

where $T^{TE} = T^{TM} = e^{i(k_{1z} - k_z)d}$ and $k_{1z} = -k_z$ (35,36) have been used. Thus we recognize that the imaginary part of the Greensfunction between the two focal points is identical to that at the same position. As a consequence $\Gamma_{12} = \Gamma_{11}$ and there is perfect sub- and superradiance, despite the fact that the distance between the focal points can be much larger than the resonance wavelength. Fig.10 illustrates the dependence of the ratio Γ_{12}/Γ_{11} on the spatial displacement of the second atom from the focal point of the first.

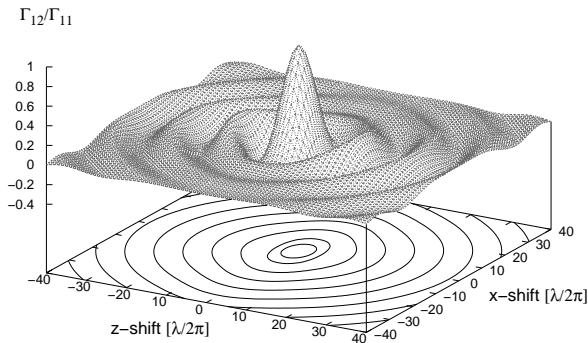


FIG. 10: Γ_{12}/Γ_{11} as function of the spatial shift, parallel ‘ x ’ and orthogonal ‘ z ’ to the surface of the LHM, of one atom out of the focus of the other one. In the focal point (0,0) perfect sub- and superradiance is obtained. Here the dipoles of both atoms are oriented in x -direction

One recognizes from fig. 10 that for the imaginary part of the Greensfunction of the ideal Veselago-Pendry lens holds

$$\text{Im}[\mathbf{G}(\mathbf{r} - 2d\mathbf{e}_z, \mathbf{r}, \omega)] = \text{Im}[\mathbf{G}(\mathbf{r}, \mathbf{r}, \omega)]. \quad (53)$$

It should be noted here that a relation similar to (53) does not exist for the real part of the Greensfunction. If this would be true the electric field pattern at the two focal points would be identical in violation of Maxwells equations. It should also be noted that relation (53) holds only within a certain range of frequencies ω due to the necessarily dispersive nature of the LHM. The limitations arising from this will be discussed in the following section.

VI. LIMITATIONS

In sections IV and V two systems involving perfect left-handed materials were discussed. We here turn to the question what are the limitations of the observed effects under more realistic conditions, i.e. when taking into account absorption losses, a finite transversal extension of the LHM slab, and dispersion of the medium.

A. Absorbing LHMs

First of all to describe a more realistic LHM one has to take into account absorption. This can easily be done by substituting the refractive index $n = -1$ of the perfect LHM by $n = -1 + in_I$, i.e. by adding an imaginary part.

For the mirror-system of sect.IV, figure 11 shows the dependence of $\Gamma^{\parallel}/\Gamma_0$ on the absorption coefficient n_I for different thicknesses of the LHM. As can be seen, the sup-

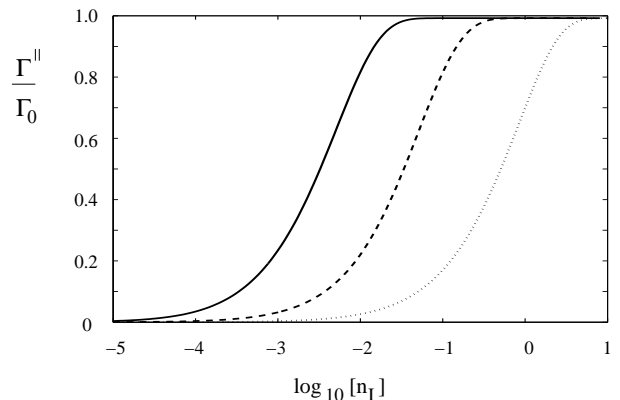


FIG. 11: $\Gamma^{\parallel}/\Gamma_0$ as function of imaginary part of refractive index n_I for $\text{Re}[n] = -1$ and different thickness d of the lens, $d = 100\lambda/2\pi$ (solid line), $d = 10\lambda/2\pi$ (dashed), and $d = 1\lambda/2\pi$ (dotted).

pression of the spontaneous emission, for atomic dipoles parallel to the mirror, decreases with increasing absorption as expected. The sensitivity to absorption is approximately exponential in $n_I d$.

In figure 12 the same is shown for the system with the lens. As expected, Γ_{12}/Γ_{11} , and therefore the effect of the sub/superradiance reduces with increasing absorption coefficients n_I . The dependence on the thickness of the lens is again exponential.

B. Finite transverse extension of the LHM

In experimental implementations the slab of LHM will always have a finite transversal extension. We therefore analyze here the dependence of the LHM-induced effects on the transversal radius of the medium. The thickness

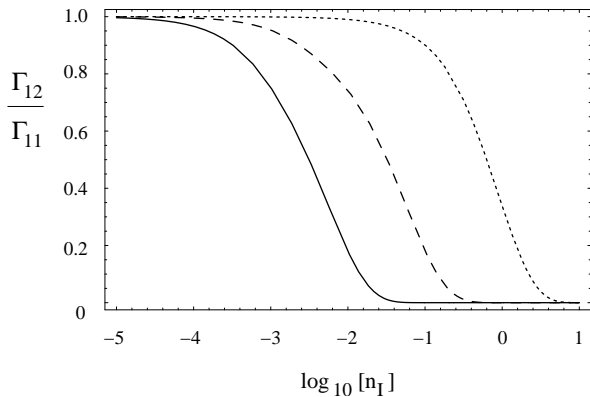


FIG. 12: Γ_{12}/Γ_{11} as function of imaginary part of refractive index n_I for $\text{Re}[n] = -1$ for different thicknesses d of the lens, $d = 100\lambda/2\pi$ (solid line), $d = 10\lambda/2\pi$ (dashed), and $d = 1\lambda/2\pi$ (dotted).

of the LHM is denoted by d , the transverse extension by a (fig. 13).

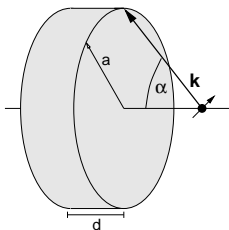


FIG. 13: Finite extension of the LHM in transverse direction.

Because of the finite radius the 1-D character of the geometry is no longer given and the Greensfunction cannot be calculated analytically. A numerical solution for the Greensfunction is also very difficult. Noting, however, that only propagating modes with $k_{\perp} \leq k$ contribute to the imaginary part of the Greensfunctions, one can obtain an estimate of the effect in the short-wavelength or ray-optics limit ($d \gg \lambda$).

For the system with the mirror this means, that for the integrand over k_{\perp} in the definition of the Greensfunction (31) one should use the expression for $\mathbf{G}_{\text{LHM}}^{00}$ only for values

$$k_{\perp} \leq k \frac{\frac{a}{d}}{\sqrt{1 + \left(\frac{a}{d}\right)^2}}. \quad (54)$$

This corresponds to angles α of the propagating modes less than $\sin \alpha = \frac{a}{\sqrt{a^2 + d^2}} = k_{\perp}/k$ (fig. 13). For greater angles the result depends strongly on whether or not the mirror has also a finite transverse extension. When the mirror has the same transverse radius a one has to use \mathbf{G}_{vac} (dashed line fig. 14), otherwise the expression for

$\mathbf{G}_{\text{LHM}}^{00}$ needs to be taken, but $n = -1$ being substituted by $n = 1$, (solid line fig. 14).

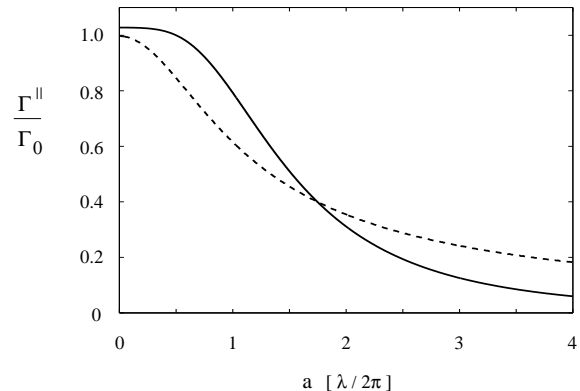


FIG. 14: $\Gamma^{\parallel}/\Gamma_0$ as function of transversal radius a of the LHM with thickness $d = 3\frac{\lambda}{2\pi}$. The mirror itself was assumed to be infinitely extended (solid) or of the same dimension as the LHM (dashed).

For the system with the lens an estimate of the effect of a finite transverse radius is given here only for a symmetric setup, i.e. the distance of both atoms to the surface of the lens being $d/2$. Under this assumption the sought result can be obtained easier than for the mirror case, since the atoms are macroscopically separated. In this case the Greensfunction $\mathbf{G}_{\text{vac}}(\mathbf{r}_1, \mathbf{r}_2)$ is essentially zero and the integration over k_{\perp} can effectively be limited to values

$$k_{\perp} \leq k \frac{\frac{a}{d}}{\sqrt{\frac{1}{4} + \left(\frac{a}{d}\right)^2}} \quad (55)$$

with the integrand being the usual expression for $\mathbf{G}^{20}(\mathbf{r}_1, \mathbf{r}_2)$. As can be seen from figure 15, even for a moderate ratio a/d a close to 100% sub/superradiance can be obtained.

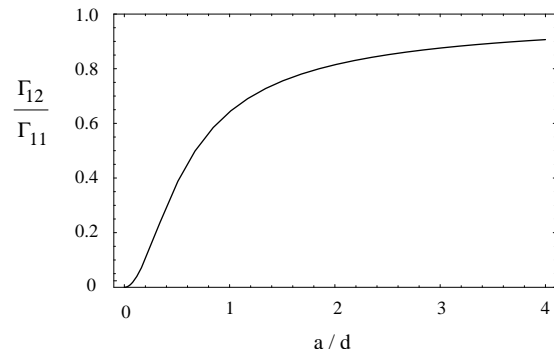


FIG. 15: Γ_{12}/Γ_{11} as function of the normalized transversal radius a/d .

C. Dispersion effects

The spontaneous emission is given by the imaginary part of the retarded Greenstensor at the transition frequency (20). Therefore the predictions of sections IV and V hold as long as the frequency range with $n = -1$ is large compared to the natural linewidth Γ .

The previous discussion suggests, that if the LHM used for the lens in sect. V has arbitrarily small losses in the frequency range of interest and also has a sufficient large transversal extension, sub- and superradiance is possible for two atoms at arbitrary distance. For causality reasons this is of course not possible. The solution of this seeming contradiction lies in the necessary dispersion of a left-handed material as discussed in sect.II. The positivity of the electromagnetic energy in a lossless LHM requires that $\frac{d}{d\omega}(\omega \text{Re}[\epsilon(\omega)]) \geq 0$, and $\frac{d}{d\omega}(\omega \text{Re}[\mu(\omega)]) \geq 0$, which implies for $n(\omega_0) = -1$:

$$\frac{d}{d\omega}n(\omega_0) \geq \frac{1}{\omega_0}. \quad (56)$$

As a consequence of the dispersion of the refractive index, the frequency window $\Delta\omega$ over which $\mathbf{G}^{20}(\omega) \approx \mathbf{G}^{00}(\omega)$ narrows with increasing thickness of the lens. When $\Delta\omega$ becomes comparable to the natural linewidth of the atomic transitions Γ_{11} , the Markov approximation implicitly used for the derivation of eq.(42) is no longer valid. To give an estimate when this happens, we note from eqs.(32)-(37) that for $d \gg \lambda$ the term in \mathbf{G}^{20} that is most sensitive to dispersion is the exponential factor $e^{i\mathbf{K}\cdot(\mathbf{r}-\mathbf{r}')}e^{i(k_{1z}-k_z)d}$. Taking into account a linear dispersion of $n(\omega)$ in this exponential factor, according to $n = -1 + \alpha(\omega - \omega_0)$, with a real value of α , while keeping the resonance values for $T^{\text{TE}}, T^{\text{TM}}$ and $R^{\text{TE}}, R^{\text{TM}}$, one finds for the Greens-tensor

$$\text{Im}[\mathbf{G}^{20}(\omega)] = \frac{k}{8\pi} \text{Re} \left[\int_0^1 d\xi (1 + \xi^2) e^{i\frac{dk_0}{\xi} \alpha(\omega - \omega_0)} \right] \hat{\mathbf{1}}. \quad (57)$$

As can be seen from Fig. 16 the spectral width $\Delta\omega$ of the Greensfunction is in this approximation of order

$$\Delta\omega \approx (k_0 d \alpha)^{-1}. \quad (58)$$

Since as mentioned above for a lossless LHM $\alpha \geq 1/\omega_0$, one arrives at

$$\Delta\omega \leq c/d. \quad (59)$$

This leads to an upper bound for the distance of the atoms. The requirement $\Delta\omega \gg \Gamma_{11}$ leads to

$$d \ll \frac{c}{\Gamma_{11}}. \quad (60)$$

This condition can easily be understood. It states that the distance between the two atoms must be small enough such that the travel time of a photon from one atom to the other is small compared to the free-space radiative lifetime.

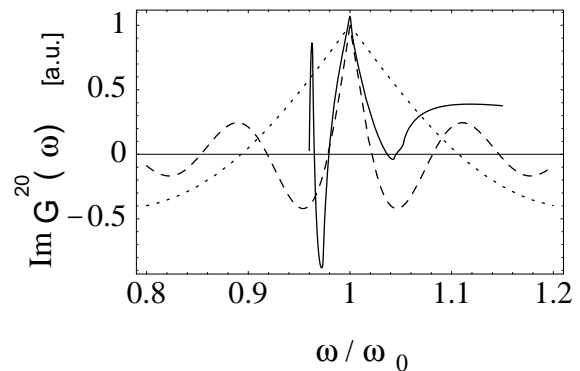


FIG. 16: $\text{Im}[\mathbf{G}^{20}(\omega)]$ following from eq.(57) for lossless LHM with $n = -1 + \alpha(\omega - \omega_0)$ for $\alpha = 45/\omega_0$ for $dk_0 = 1$ (dashed), 0.2 (dotted). Also shown is the numerically calculated spectrum for a specific causal model for $n(\omega)$ with resonances of $\epsilon(\omega)$ and $\mu(\omega)$ below ω_0 . $n(\omega)$ was chosen such that $\text{Re}[n(\omega_0)] = -1$ and $\alpha = 45/\omega_0$. The central structure is well represented by the linear-dispersion approximation (57). Furthermore a narrowing of the spectral width with increasing thickness is apparent.

VII. SUMMARY

In the present paper we have studied the interaction of an isolated atom or a pair of atoms with the quantized electromagnetic field in the presence of media with negative index of refraction. An expression for the rate of spontaneous emission of an atom embedded in a LHM was derived (see also [15]) which is a generalization of the Glauber-Lewenstein result [17] to magneto-dielectric media. We have shown that the negative optical path length occurring in left-handed materials can be used to induce strong QED effects over large distances, which in vacuum occur only on sub-wavelength length scales. Considering an isolated atom in front of a perfect mirror with a layer of LHM of thickness d we found an interesting modification of the Purcell effect. Spontaneous emission was found to be completely suppressed for an atom placed at distance $2d$ from the mirror in vacuum. It was shown furthermore that two atoms in the focal points of a Veselago-Pendry lens, consisting of a parallel slab of ideal LHM, display perfect sub- and superradiance. A principle limitation of the involved length scales is given only by the intrinsic dispersion of left handed materials which prevents the strong radiative coupling over distances larger than the propagation distance of light corresponding to the free-space radiative decay time. We anticipate that the unusual property of LHM to lead to negative optical path length will have a number of interesting applications an example being zero-optical length resonators. On the other hand much of the present discussion is still only of academic interest since until now no low-loss negative index materials are known for the interesting case of optical frequencies.

-
- [1] Purcell, E.M., 1946, Phys. Rev. **69**, 681.
- [2] Kleppner, D., 1971, Atomic Physics and Astrophysics, edited by M. Chretien and E. Lipworth (New York: Gordon and Breach).
- [3] Hulet, R.G., Hilfer, E.S., and Kleppner D., 1985, Phys. Rev. Lett. **55**, 2317.
- [4] Goy, P., Raimond, J.M., Gross, M., and Haroche, S., 1983, Phys. Rev. Lett. **50**, 1903.
- [5] Vaidyanathan, A.G., Spencer, W.P., and Kleppner, D., 1981, Phys. Rev. Lett. **47**, 1592.
- [6] Dobiashch, P., and Walther, H., 1985, Ann. Phys. (Paris), **10**, 825.
- [7] Drexhage, K.H., 1974, Progress in Optics, edited by E. Wolf, (Amsterdam: North-Holland).
- [8] Yamamoto, Y., 1991, Opt. Comm. **80**, 337.
- [9] Yablonovich, E., 1987, Phys. Rev. Lett. **58**, 2059.
- [10] John, S., and Quang, T., 1994, Phys. Rev. A **50**, 1764.
- [11] Veselago, V.G., 1968, Sov. Phys. Usp. **10**, 509.
- [12] Pendry, J.B., 2000, Phys. Rev. Lett. **85**, 3966.
- [13] Dicke, R.H., 1954, Phys. Rev. **93**, 99.
- [14] Nienhuis, G., and Alkemande, C.Th.J., 1976, Physica C **81**, 181.
- [15] Dung, Ho Trung, Buhmann S.Y., Knöll, L., Welsch, D.-G., Scheel, S., and Kästel, J., 2003, Phys. Rev. A **68**, 043816.
- [16] Kästel, J., 2003, diploma thesis, TU Kaiserslautern.
- [17] Glauber, R.J., Lewenstein, M., 1991, Phys. Rev. A **43**, 467.
- [18] Knöll, L., Scheel, S., Welsch, D.G., 2001, QED in Dispersing and Absorbing Dielectrics in Coherence and Statistics of Photons and Atoms, ed. J. Peřina, (New York: John Wiley).
- [19] Li, L.W., Kooi, P.S., Leong, M.S., Yeo, T.S., 1994, IEEE Trans. Microwave Theory Tech. **42**, 2302.
- [20] Morawitz, H., 1969, Phys. Rev. **187**, 1792.
- [21] Tsang, L., Kong, J.A., and Shin, R.T., 1985, Theory of Microwave Remote Sensing, (New York: John Wiley & Sons).

Information about corresponding author

M. Fleischhauer

Fachbereich Physik
Technische Universität Kaiserslautern
D-67663 Kaiserslautern

phone: ++ 49 631 205 3206

fax: ++ 49 631 205 3907

email: mfleisch@physik.uni-kl.de